

See discussions, stats, and author profiles for this publication at: <https://www.researchgate.net/publication/234904336>

The Application of Magneto Inductive Sensors for Non-Destructive Testing of Steel Reinforcing Bars Embedded Within Pre-Stressed and Reinforced Con....

Article · March 2006

DOI: 10.1063/1.2184672

CITATIONS

3

READS

126

5 authors, including:



Diego Benitez

Universidad San Francisco de Quito (USFQ)

114 PUBLICATIONS 1,795 CITATIONS

[SEE PROFILE](#)



S. Quek

The University of Manchester

29 PUBLICATIONS 258 CITATIONS

[SEE PROFILE](#)



Patrick Gaydecki

The University of Manchester

155 PUBLICATIONS 1,518 CITATIONS

[SEE PROFILE](#)



V. Torres

The University of Manchester

12 PUBLICATIONS 55 CITATIONS

[SEE PROFILE](#)

Some of the authors of this publication are also working on these related projects:



CEDIA - CEPRA [View project](#)



Electromyography and kinesiology [View project](#)

THE APPLICATION OF MAGNETO INDUCTIVE SENSORS FOR NON-DESTRUCTIVE TESTING OF STEEL REINFORCING BARS EMBEDDED WITHIN PRE-STRESSED AND REINFORCED CONCRETE

D.S. Benitez, S. Quek, P. Gaydecki, V. Torres and B. Fernandes

Sensing, Imaging and Signal Processing Group (SISP), School of Electrical and Electronic Engineering,
The University of Manchester, PO Box 88, Manchester M60 1QD, United Kingdom

ABSTRACT. This paper demonstrates the feasibility of using solid-state magneto-inductive probes for detecting and imaging of steel reinforcing bars embedded within pre-stressed and reinforced concrete. Changes in the inductance of the sensor material are directly proportional to the strength of the measured magnetic field parallel to the sensor. Experimental results obtained by scanning steel bars specimens are presented. General performance characteristics and sensor output limitations are investigated by using different orientations, sensing distance, excitation intensity, bar sizes and geometries.

Keywords: Inductive sensor, GMI, Metal detection

PACS: 85.75.Ss, 81.70.-q, 07.55.Ge.

INTRODUCTION

Solid-state, thick and thin film magnetic sensors are being increasingly used to measure weak magnetic fields, such as the earth magnetic field. In general, these devices are entirely non-hazardous and inexpensive. Although the degree of sensitivity achieved by solid state magnetic sensors such as magneto inductance, giant magneto impedance (GMI) and giant magneto resistance (GMR) devices is not as yet comparable to superconducting quantum interference devices (SQUIDS), they have sensitivities in the range of nanoTeslas (nT) and are certainly superior to modalities based on the Hall Effect [1]. Furthermore, important advantages of GMI and GMR sensors such as high resolution, small size, quick response, high sensitivity to a well defined axis, noise immunity, temperature stability, low power consumption and repeatability make them suitable for robust detection system design.

In an earlier publication, the authors studied the possibility of using GMR sensors for imaging steel reinforcing bars in concrete [2]. Here, the possibility of using commercially available magneto inductive sensors for the same purpose is investigated.

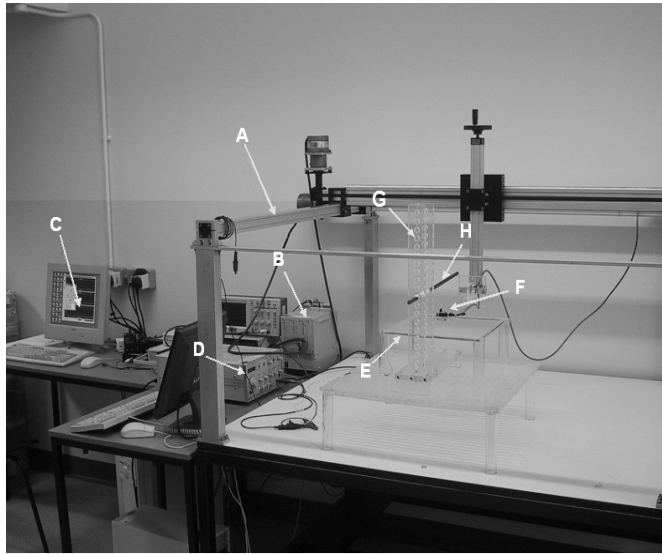


FIGURE 1. Experimental Setup: A. X-Y Scanner system, B. Motor controller and power drivers, C. PC for control and data acquisition, D. Power generator, E. 30x30cm coil, F. Sensor probe, G. Variable height support, H. Reinforcement bar target.

METHOD

Experimental Setup

Figure 1 shows the setup of experimental equipment. The excitation magnetic field was produced by using a DC power supply (0.5-1.5 A) and a 300×300 mm square coil (1 Ω resistance) with an air-core. The optimum dimensions of the coil were determined by modelling simulation using a 3D commercial available software package called FARADAY 3D which is based on the boundary element method (BEM) [3].

The Sensor Probe

Three MI sensors (PNI Corp. PNI Sen-s65) [4] were used in a 3-axis configuration probe. Each sensor unit sensed the magnetic field parallel to the orientation of the sensor. The 3 sensors were mounted in 3D spatial orientation in order to measure the B_x , B_y and B_z components of the magnetic flux density. Each sensor had a total field range from -11 to +11 Gauss, with a typical resolution of around 0.015 μ T. The reading from each MI sensor was performed and digitized by using an Application Specific Integrated Circuit (ASIC) module and a 16-bit microprocessor and then sent to a computer via the RS 232 interface. The ASIC (PNI 11096) [4] incorporates all the circuitry required to implement a temperature and noise stabilized oscillator/counter circuit. It also provides a SPI interface for communication with the microprocessor.

A smoothing algorithm such as the method of moving averages was used for further improvement of the MI sensors output and for reducing noise before image generation. The sensor probe was moved by a laboratory-based motorised x-y scanner controlled by a computer. A scan step of 1.1 mm was used for both axes.

Experimentation

Several 2D scans were conducted in order to determine the performance and limitations of the sensor. In a first instance a 10 mm bar was positioned as metal target located at different deep positions between 50 to 100 mm from the plane of the coil using a variable height support system. The sensor probe was located at about 30 mm from the plane of the coil and in the same side with the metal target. The optimum position of the sensor probe was also determined by model simulation. The magnetic field in the coil was generated with different current intensities ranging from 0.5 to 1.5 A.

An additional test was also conducted by placing the sensor at the opposite side of the coil in order to determine if the probe was also capable of detecting and imaging the metal target at different deeps. The results obtained are summarised in the next section.

RESULTS AND DISCUSSION

Validation of the Modelling

The distribution of magnetic flux density in the 3 axes generated by the coil (B_x , B_y and B_z) were measured within the range of mm every 1.1 mm step. All the measurements were corrected by measuring and subtracting background magnetic fields such as terrestrial magnetism or other magnetic fields caused by electrical machinery near the MI sensor probe in the calibration process. Figure 2 shows the results of the B_z magnetic flux density distribution obtained by simulation and sensor measurement 20 mm from the plane of the coil. As it can be seen from the plots in Figure 2, the experimental measurement qualitatively matches the model prediction. Similarly, Figure 3 shows the results for the B_y . In this case, although experimental measurement looks similar to the model prediction, the line scan at the horizontal centre of the coil presents oscillations due to mechanical vibrations of the arm resulting from the slow scanning speed and the need to use a sparse dataset for image generation. Although this is a limitation of image generation, it is also a good indication of the high sensitivity of the sensor.

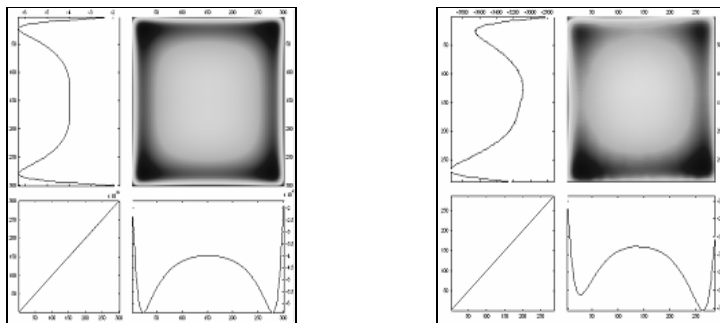


FIGURE 2. Simulation prediction (left) and experimental magnetic field (right) in B_z component at 20 mm from the plane of the coil. Plots at the top left of each graph show the line scan values at the vertical centre of the coil. The plot at the bottom right of each graph shows the line scan at the horizontal centre of the coil. The plot at the top right of each graph shows the 2D magnetic flux density distribution of the coil.

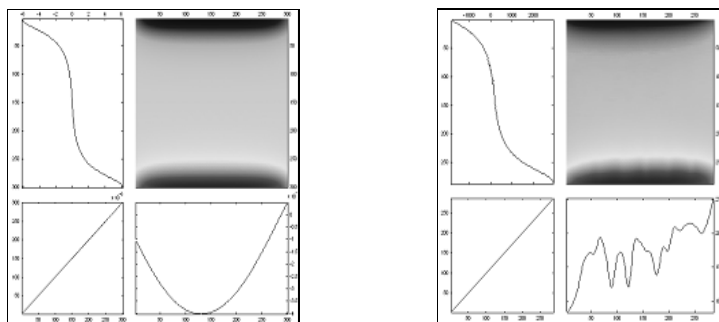


FIGURE 3. Simulation prediction (left) and experimental measurement (right) for the magnetic field in the B_y component at 30 mm from the plane of the coil. The plots at the top left of each graph show the line scan values at the vertical centre of the coil. The plot at the bottom right of each graph shows the line scan at the horizontal centre of the coil. The plot at the top right of each graph shows the 2D magnetic flux density distribution of the coil.

Rebar Detection

Two dimensional scans of the magnetic field of the coil alone and after distortion in the field caused by the metal target were taken using the same methodology described above. Images were generated by subtracting the magnetic field generated by the coil alone from the measurement of the influence of the metal target in the magnetic field of the coil. All measurement points were standardized and normalized in mm. The distribution of the component of the magnetic flux density (B_z) of the coil alone and the distortion in this field caused by the presence of the metal target are shown in Figures 4 and 5.

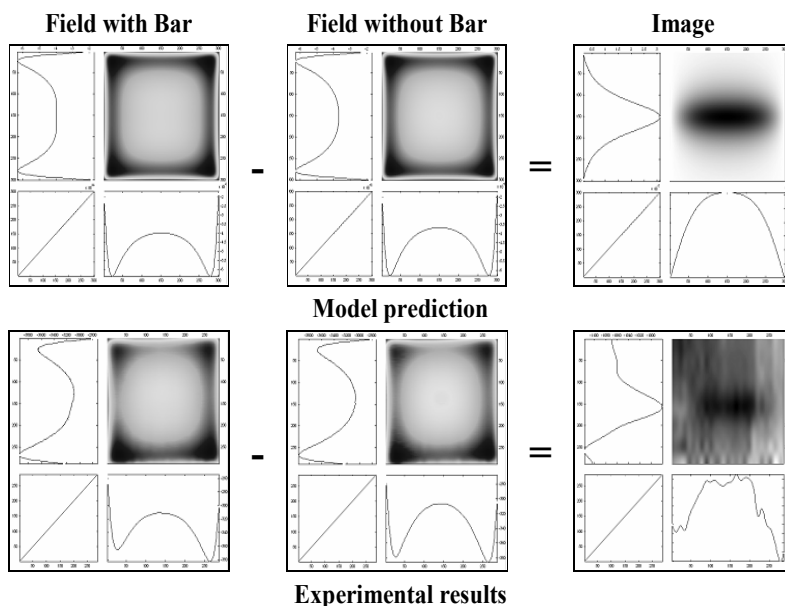


FIGURE 4. 2D Image generation of a 10mm bar placed at 75 mm from the plane of the coil. The sensor was placed at the same side as the bar. The plots at the top show the simulation predictions for the magnetic field in the B_z component at 20 mm from the plane of the coil. The plots at the bottom show the experimental measurements.

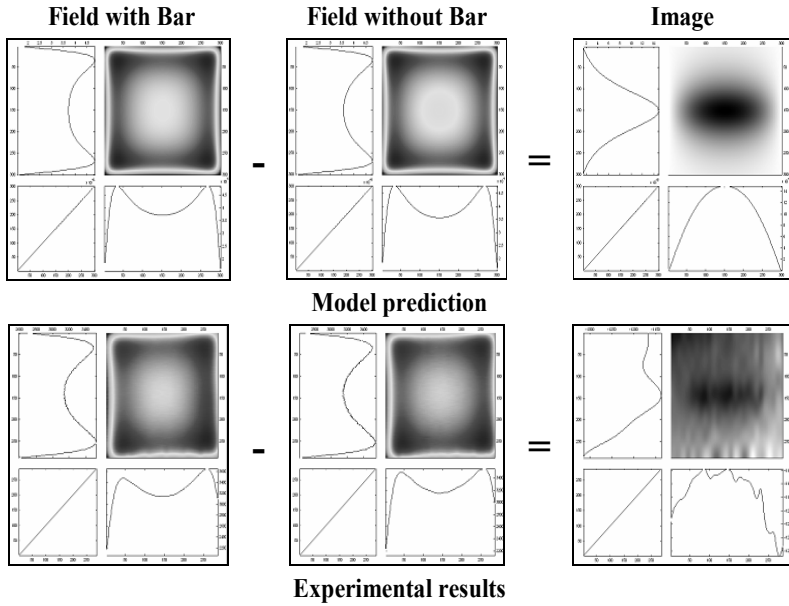


FIGURE 5. 2D Image generation of a 10mm bar placed at 100 mm from the plane of the coil. The sensor was placed at opposite same side of the bar. The plots at the top show the simulation predictions for the magnetic field in the B_z component at 30 mm from the plane of the coil. The plots at the bottom show the experimental measurements.

As determined by simulation, [3] the B_z component is the most favourable for image generation as its image is easy to interpret and can be readily reconstructed to generate the geometry of the bar. It can also be seen that the results obtained by the sensor probe agree with the simulation prediction.

Figure 6 shows the image obtained by positioning the sensor on the opposite side of the meal bar. The images obtained could also be further improved by image processing techniques such as 2D low high and low pass filtering.

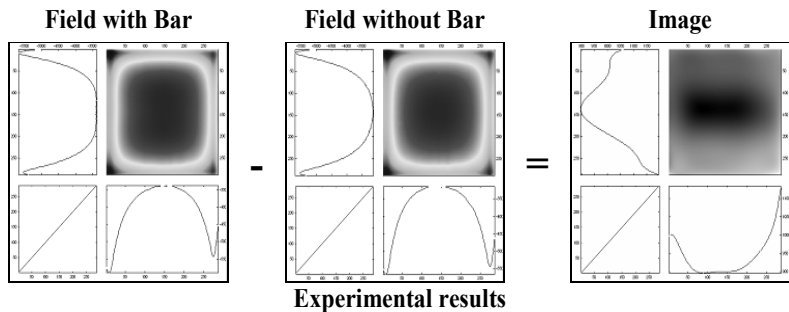


FIGURE 6. 2D Image generation of a 10mm bar placed 100 mm from the plane of the coil. The sensor is placed opposite the bar. The plots show the experimental measurements for the magnetic field in B_z component at 30 mm from the plane of the coil.

CONCLUSION

Magneto-inductive sensors have proved their suitability for use in a scanning system oriented to imaging steel bars embedded in concrete. Simulated results have qualitatively predicted the experimental outcomes. Initial simulations and experimental results encourage further development of the system. The resolution and sensitivity of the magneto-inductive sensors are adequate for the purpose of detecting metal bars. With specifically designed circuitry, the sensor could be used in an array of sensors. Compared to other developments, the magneto-inductive sensors show promising improvements in spatial resolution.

ACKNOWLEDGEMENT

The authors wish to express their gratitude to the Engineering and Physical Sciences Research Council in the UK for financially supporting this work.

REFERENCES

1. A.E. Mahdi, L. Panina, D. Mapps, *Sensors and Actuators A* **105**, 271–285 (2003).
2. V. Torres, P. Gaydecki, G. Miller, B. Fernandes and M. Zaid, “The use of Magnetoresistors for Imaging Steel Bars in Concrete”, in *Review of Progress in Quantitative Nondestructive Evaluation 24B*, edited by D. O. Thompson and D. E. Chimenti, AIP Conference Proceedings vol. 760, American Institute of Physics, Melville, NY, 2005, pp. 1453-1460.
3. S. Quek , D. Benitez, P. Gaydecki, and V. Torres, “Studies on geometries for inducing homogeneous magnetic field in the application of real time imaging of steel reinforcing bars embedded within pre-stressed and reinforced concrete”, in *Review of Progress in Quantitative Nondestructive Evaluation 25B*, edited by D. O. Thompson and D. E. Chimenti, AIP Conference Proceedings vol. 760, American Institute of Physics, Melville, NY, 2005.
4. PNI Corporation, Sen-S65 SMT Sensor and 1096 Driver ASIC, Sensor products. www.pnicorp.com